ELSEVIER

Biophysical Chemistry 98 (2002) 217–232

Biophysical Chemistry

www.elsevier.com/locate/bpc

Changes in the abnormal α-subunit upon CO-binding to the normal β-subunit of Hb M Boston: resonance Raman, EPR and CD study

Shigenori Nagatomo[a], Yayoi Jin[b], Masako Nagai[b], Hiroshi Hori[c], Teizo Kitagawa[a,*]

[a]*Center for Integrative Bioscience, Okazaki National Research Institutes, Myodaiji, Okazaki, Aichi 444-8585, Japan*
[b]*School of Health Sciences, Kanazawa University Faculty of Medicine, Kanazawa 920-0942, Japan*
[c]*Division of Biophysical Engineering, Graduate School of Engineering Science, Osaka University, Toyonaka, Osaka 560-8531, Japan*

Received 12 October 2001; received in revised form 8 February 2002; accepted 8 February 2002

Abstract

Heme–heme interaction in Hb M Boston (Hisα58→Tyr) was investigated with visible and UV resonance Raman (RR), EPR, and CD spectroscopies. Although Hb M Boston has been believed to be frozen in the T quaternary state, oxygen binding exhibited appreciable co-operativity ($n=1.4$) and the near-UV CD spectrum indicated weakening of the T marker at pH 9.0. Binding of CO to the normal β-subunit gave no change in the EPR and visible Raman spectra of the abnormal α-subunit at pH 7.5, but it caused an increase of EPR rhombicity and significant changes in the Raman coordination markers as well as the Fe(III)-tyrosine related bands of the α-subunit at pH 9.0. The UVRR spectra indicated appreciable changes of Trp but not of Tyr upon CO binding to the α-subunit at pH 9.0. Therefore, we conclude that the ligand binding to the β heme induces quaternary structure change at pH 9.0 and is communicated to the α heme, presumably through Hisβ92→Trpβ37→Hisα87. © 2002 Elsevier Science B.V. All rights reserved.

Keywords: Hemoglobin; M Boston; Quarterly structure; Resonance Raman; EPR; CD; UV resonance Raman

1. Introduction

Hemoglobins (Hb) M have an abnormal chain in either the α- or β-subunit of the $\alpha_2\beta_2$ tetramer, yielding a natural valency-hybrid Hb under physiological conditions, that is, a ferric heme in the abnormal subunit and a ferrous heme in the normal subunit. There are four kinds of Hb Ms in which either the proximal or the distal histidine is replaced by tyrosine in the α- or β-subunit. They are named Hb M Iwate (Hisα87→Tyr), Hb M

Abbreviations: Hb A, hemoglobin A; COHb A, carbonmonoxy Hb A; IHP, inositolhexakisphosphate; RR, resonance Raman; UVRR, ultraviolet resonance Raman; $\alpha_2^{Co}\beta^{deoxy}$, α-Co-β-Fe-deoxy hybrid Hb; $\alpha_2^{Mmet}\beta_2^{deoxy}$, α-Fe(III)-β-Fe(II)-deoxy Hb M Boston; $\alpha_2^{Mmet}\beta_2^{CO}$, α-Fe(III)-β-Fe(II)-CO Hb M Boston; $\alpha_2^{Ni}\beta_2^{deoxy}$, α-Ni-β-Fe-deoxy Hb; $\alpha_2^{deoxy}\beta_2^{Ni}$, α-Fe-deoxy-β-Ni Hb; 5c-hs, five-coordinate high-spin; 6c-hs, six-coordinate high-spin; 6c-ls, six-coordinate low-spin; PPIXDBE, protoporphyrin-IX dibenzylester.

*Corresponding author. Tel.: +81-564-55-7340; fax: +81-564-55-4639.

E-mail address: teizo@ims.ac.jp (T. Kitagawa).

PII: S0301-4622(02)00103-5

Boston (Hisα58→Tyr), Hb M Hyde Park (Hisα92→Tyr), and Hb M Saskatoon (Hisβ63→Tyr). Hb Ms have properties different from those of normal Hb A as the replaced tyrosine is coordinated to the abnormal heme. Hb M Iwate and Hb M Boston, whose α-chains are abnormal, have very low oxygen affinity and show neither cooperativity nor Bohr effect at neutral pH [1,2]. Hb M Hyde Park and Hb M Saskatoon, whose β-chains are abnormal, have normal oxygen affinity and decreased but significant co-operativity [3,4]. Although the residues constituting the subunit interfaces are the same between Hb Ms and Hb A, the apparent heme–heme interaction is distinct between whether the replacement is present in the vicinity of heme of the α or β subunit.

The co-operative oxygen binding of Hb A has been explained in terms of reversible transition between the two quaternary structures [5], called T (tense) with low oxygen affinity and R (relaxed) states with high oxygen affinity [6,7]. The largest structural differences between the T and R structures, revealed by X-ray crystallographic analysis [8], are located in the $\alpha_1-\beta_2$ subunit interface, where resets of hydrogen bonds and salt-bridges take place upon ligand binding or dissociation. The appearance of a heme–heme interaction is different when a ligand is bound to the α- or β-subunit, but such feature cannot be clarified with normal Hb, because the α- and β hemes cannot be distinguished from each other. A method to investigate a more detailed mechanism of the heme–heme interaction is to use a Hb which allows ligand binding only to the α- or β-heme. Hb Ms are suitable to this purpose. Although Hb M Iwate and Hb M Boston, having an abnormal α chain, hardly show co-operativity in oxygen binding, it does not always mean depletion of the $\alpha_1-\beta_2$ intersubunit interactions. Presumably, binding of two ligands to normal β-subunits at pH 7 is not sufficient to change a quaternary structure from T to R. However, for the Co–Fe hybrid Hb, the subunit communication is present and observed upon binding of two ligands. For instance, CO cannot bind to the α-subunit in the $\alpha_2^{Co}\beta_2^{deoxy}$ hybrid Hb similar to Hb M Iwate and Hb M Boston, but binding of CO to its β-heme causes a low field shift of ^{1}H NMR of proximal Hisα87 [9], indicating that the ligand binding in the β-subunit is communicated to the proximal His of the α-subunit and to have made the Co–His bond-length shorter.

The Fe(III) heme in the α-subunit of Hb M Boston allows us to measure EPR signals and thus to monitor a change in an electronic state of the Fe(III) heme in the α-subunit upon binding of a ligand to the ferrous heme of the partner β-subunit. So far it is known that anisotropy of *g* values changes upon oxygenation to the normal α-heme of Hb M Hyde Park at pH 7 [10]. Proton NMR studies of Hb M Milwaukee, in which Valβ67 is replaced by Glu and therefore, the β-heme always remains in the ferric state, have shown that the CO and O_2 binding to the normal α-subunit can affect the hyperfine-shifted ^{1}H resonances of the abnormal β-subunit [11,12]. These data indicate the presence of the communication from the α- to β-subunit during the ligation process of these Hbs, although direct electrostatic interaction between the two hemes is unlikely as their distance is approximately 250 pm. To answer a question, how the effect of O_2-binding to one heme is communicated to the other heme, we investigated, in this study, the communication from the β- to α-subunit upon ligand binding to the β-subunit by monitoring the EPR and visible RR spectra of the α-heme together with the measurement of UVRR and CD spectra reflecting the $\alpha_1-\beta_2$ subunit contacts.

2. Experimental procedures

2.1. Sample preparations

Hb A was purified from fresh human blood by a preparative isoelectric focusing electrophoresis [13]. Hb M Boston was separated from Hb A on Amberlite CG-50 column pre-equilibrated with 0.05 M phosphate buffer pH 7.0. After Hb A was washed out of the column with the same buffer, Hb M Boston remaining on the column was eluted with 0.2 M phosphate buffer, pH 7.0 [14]. $\alpha_2^{Mmet}\beta_2^{deoxy}$ and $\alpha_2^{Mmet}\beta_2^{CO}$ of Hb M Boston were prepared by repetition of deaeration followed by flushing with pure N_2 and flowing with CO.

2.2. EPR spectra

EPR measurements were carried out at X-band (9.35 GHz) microwave frequency using a Varian E-12 spectrometer with 100 kHz field modulation [15]. An Oxford flow cryostat Dewar (ESR-900) was used for measurements at 5 K. The microwave frequency was calibrated with a microwave frequency counter (Takeda Riken, model TR5212). The magnetic field strength was determined by an NMR field meter EFM-2000AX (ECHO Electronic Co. Ltd., Japan). EPR spectra were recorded with a microwave power of 5 mW and a field modulation width of 0.5 mT (tesla). EPR signal intensity was directly proportional to the amounts of Fe(III) hemes in Hbs under these conditions.

2.3. Visible resonance Raman spectra

Visible resonance Raman spectra were excited with the 413.1 nm line of a Kr laser (Model 2060, Spectra Physics) and the 488.0 nm line of an Ar laser (Model GLG3200, NEC), and detected with a liquid nitrogen cooled CCD detector (Model CCD3200, Astromed and Model LN/CCD-1300-PB, Princeton Instruments) attached to a 100-cm single polychromator (Model MC-100DG, Ritsu Oyo Kogaku). The slit width and slit height were set to be 200 μm (488 nm) or 150 μm (413.1 nm) and 20 mm, respectively. The spectral slit-widths are 6.6 (488 nm) and 7.1 cm^{-1} (413.1 nm). The wavenumber width per one channel (resolution) of the detector is 0.73 (488 nm) and 0.82 cm^{-1} (413.1 nm) under this condition. The laser power was made as low as possible and practically they were 50 (488 nm) and 0.25 mW (413.1 nm) at the sample point.

For the experiments with the 488.0 and 413.1 nm excitation, 600 and 150 μl, respectively, of the 200 μM (heme) Hb solution were put into a spinning cell. Dissociation of CO by the probe laser was monitored by the ν_4 band, which appears at $\sim$1355 and $\sim$1370 cm^{-1} for photodissociated and non-dissociated forms, respectively. All measurements were carried out at room temperature with a spinning cell (1000 r.p.m.). Raman shifts were calibrated with indene and accuracy of the peak positions of Raman bands was ± 1 cm^{-1}. Integrity of each form was confirmed with visible absorption spectrum after RR measurements.

2.4. Ultraviolet resonance Raman spectra

UVRR spectra were excited by a XeCl excimer laser-pumped dye laser (LPX120 and SCANMATE, Lambda Physik). The 308 nm line from a XeCl excimer laser (operated at 100 Hz) was used to excite coumarin 480, and the 470 nm output from the dye laser was frequency-doubled with a β-BaB_2O_4 crystal to generate 235 nm pulses. The Raman excitation light (15 μJ/pulse) was introduced to the area of 0.2×3 mm^2 of sample cell from the lower front side. The scattered light was dispersed with an asymmetric double monochromator (Spex 1404) in which the gratings in the first and second dispersion steps were of the first order use of a 2400 grooves/mm (holographic), and of the second order use of a 1200 grooves/mm (machine-ruled, 500 nm blaze) grating, respectively [16], and detected by an intensified photodiode array (PC-IMD/C5222-0110G).

Approximately 150 μl of Hb sample (200 μM in heme) in Tris–Cl buffer was put into a spinning cell made of a synthetic quartz EPR tube with a diameter of 5 mm [17]. Just before the measurement of UVRR spectra, Na_2SO_4 was added to the samples with the final concentration of 0.1 M as an internal intensity standard for Raman spectra. It was confirmed that the addition of sulfate did not cause any apparent Raman spectral change for the states examined in this study, although its use in Raman experiments was warned against due to possible tertiary structure change [18]. Other details of UV Raman measurements were described previously [19].

2.5. Circular dichroism spectra

CD spectra were measured with a Jasco J-725 spectropolarimeter at 25 °C with a cell path-length of 2 mm. The instrument was calibrated with (+)-10-camphorsulfonic acid. Spectra were recorded with a scan speed of 50 nm/min, a slit-width of 1 nm, and a detector response time of 1 s, and 20 scans were averaged into a single spectrum. The observed spectra were corrected by

subtraction of the solvent spectrum obtained under the identical condition. The results are represented with the unit of $\Delta\varepsilon$ (M^{-1} cm^{-1}) per mole of protein (in heme basis). The spectrum of Hb A was measured in individual series of measurements as a control. All samples used were 50 μM (in heme) in 0.05 M Tris–Cl buffer.

2.6. Absorption spectra

Absorption spectra of Hb A and Hb M Boston were measured for both deoxy and CO forms at pH 7.5 and 9.0 with a Hitachi U-3210 spectrophotometer. The sample concentration was 10 and 200 μM for the B and Q band regions, respectively.

2.7. Oxygen equilibrium

Oxygen equilibrium curves were determined by a spectroscopic method according to Sugita and Yoneyama [20] for the Hb solution with the concentration of 50–60 μM (in heme) in 0.05 M Tris–Cl buffer containing 0.1 M NaCl. Hb was deoxygenated by repetition of alternate evacuation and flushing with the Q gas (helium/isobutane = 99.05/0.95) in a Thunberg-type cell with 1-cm light path. A pH value of the Hb solution was determined at the end of experiment.

3. Result

Fig. 1 shows the $g_\perp$ region of EPR spectra of metHb A (a), $\alpha_2^{Mmet}\beta_2^{deoxy}$ and $\alpha_2^{Mmet}\beta_2^{CO}$ of Hb M Boston at pH 7.5 (b) and those at pH 9.0 (c). The EPR spectra of Fe(III) high-spin hemes generally give rise to the pattern of axial symmetry with peaks at $g_\perp = 6$ and $g_{//} = 2$. In fact, the $g_\perp$ spectrum of metHb A gives a single peak at $g = 6$, but that of Hb M Boston exhibits splitting into $g_1 = 6.32$ and $g_2 = 5.76$ at pH 7.5. It means the presence of anisotropy in the α heme plane in Hb M Boston. The anisotropy of the α heme in the $\alpha_2^{Mmet}\beta_2^{deoxy}$ state is almost the same between pH 7.5 [(b), solid line)] and 9.0 [(c), solid line]. Upon binding of CO to the β heme, the splitting is almost the same between $\alpha_2^{Mmet}\beta_2^{deoxy}$ [(b), solid line] and $\alpha_2^{Mmet}\beta_2^{CO}$ [(b), broken line] at pH 7.5, but additional new rhombic signals with larger splitting

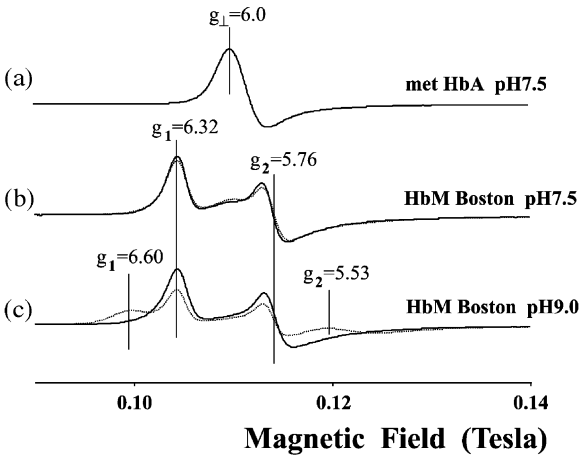

Fig. 1. EPR spectra of metHb A at pH 7.5 (a), Hb M Boston $\alpha_2^{Mmet}\beta_2^{deoxy}$ (solid line) and $\alpha_2^{Mmet}\beta_2^{CO}$ (broken line) at pH 7.5 (b), and Hb M Boston $\alpha_2^{Mmet}\beta_2^{deoxy}$ (solid line) and $\alpha_2^{Mmet}\beta_2^{CO}$ (broken line) at pH 9.0 (c). All the EPR spectra were recorded at 5 K. All samples are equilibrated with 0.05 M Tris–Cl buffer, containing 0.1 M NaCl, and the concentration of Hb is 200 μM in heme.

($g_1 = 6.60$ and $g_2 = 5.53$) appeared at pH 9.0 [(c), broken line]. Anisotropy of the *g*-value is generally represented in terms of rhombicity, that is, $[(g_1 - g_2)/16 \times 100]$. In this case, the rhombicity is changed from 3.50 ($\alpha_2^{Mmet}\beta_2^{deoxy}$) to 6.69 ($\alpha_2^{Mmet}\beta_2^{CO}$) by binding of CO to the β heme at pH 9.0. The Fe(III) low-spin signal was not detected for neither $\alpha_2^{Mmet}\beta_2^{deoxy}$ nor $\alpha_2^{Mmet}\beta_2^{CO}$ at pH 7.5 and 9.0.

Fig. 2 shows the absorption spectra of Hb M Boston at pH 7.5 and 9.0. The deoxy form [(a) and (b)] has a Soret peak at 406 nm with a shoulder at 425 nm, and the CO form [(c) and (d)] has a main peak at 420 nm with a shoulder at 406 nm, while the spectra in the Q band region are in agreement with previous measurements [21]. The spectral change is due to the contribution of the ferrous β-heme upon the change from the deoxy (425 nm shoulder) to the CO form (420 nm). The pH difference spectra between pH 7.5 and pH 9.0 observed for $\alpha_2^{Mmet}\beta_2^{deoxy}$ (e) and $\alpha_2^{Mmet}\beta_2^{CO}$ (f) indicate that their patterns are alike, but the magnitude is larger for $\alpha_2^{Mmet}\beta_2^{CO}$ than for $\alpha_2^{Mmet}\beta_2^{deoxy}$. The inset shows the same set of spectra in the Q band region obtained with more

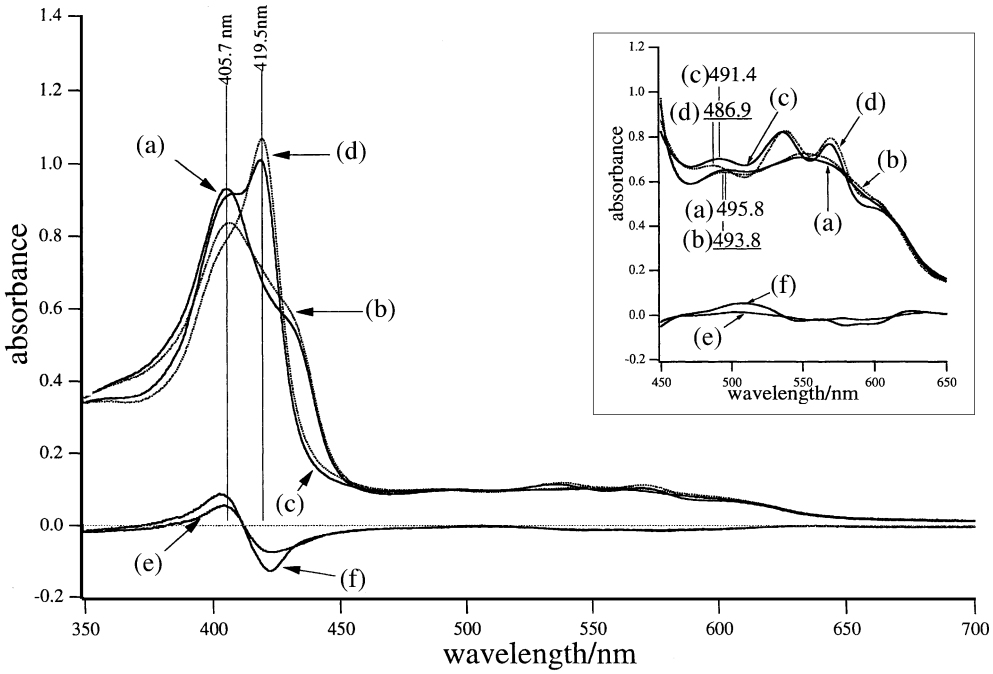

Fig. 2. Absorption spectra of Hb M Boston $\alpha_2^{Mmet}\beta_2^{deoxy}$ at pH 7.5 (a, –) and $\alpha_2^{Mmet}\beta_2^{deoxy}$ at pH 9.0 (b, …), $\alpha_2^{Mmet}\beta_2^{CO}$ at pH 7.5 (c, –), and $\alpha_2^{Mmet}\beta_2^{CO}$ at pH 9.0 (d, …), and their difference spectra; e [(a) minus (b)], and f [(c) minus (d)]. All samples are equilibrated with 0.05 M Tris–Cl buffer, containing 0.1 M NaCl. The concentration of Hb is 10 and 200 μM in heme and the cell thickness is 10 and 2 mm, for the spectra in the main frame and inset, respectively, while the inset shows the spectra only between 450 and 650 nm.

concentrated solutions. One broad peak appeared for the deoxy form [(a) and (b)], but two peaks (β- and α bands) appeared for the CO form [(c) and (d)], and their pH difference is larger for the CO form (f) than for the deoxy form (e), although their magnitudes are so small. Note that a positive peak is present at approximately 520 nm for the CO form (f), meaning the decrease of a CT absorption at pH 9.0 than pH 7.5.

According to Suzuki et al. [2], Hb M Boston exhibits very low oxygen affinity, low co-operativity, and no Bohr effect between pH 6 and 8. Fig. 3 shows the oxygen equilibrium curves of Hb M Boston at pH 7 and 9 in comparison with Hb A at pH 7. Raising pH for Hb M Boston resulted in a slightly increased oxygen affinity from $P_{50}=$ 27.5 (pH 7) to 21.5 mmHg (pH 9), and an increased Hill's coefficient from $n=1.2$ (pH 7) to 1.4 (pH 9). The values at pH 7 agree with those reported by Suzuki et al. [2]. As only two subunits can bind oxygen in Hb M Boston, the maximal value of n is 2.0 for Hb M Boston rather than 4.0 for Hb A. Considering $n=2.8$ for Hb A, the increase in the n-value of Hb M Boston from 1.2 to 1.4 seems to be significant, reflecting some change in the $\alpha_1-\beta_2$ contacts.

Fig. 4 shows the 413.1 nm excited resonance Raman (RR) spectra of Hb M Boston at pH 7.3 [(a) and (c)] and pH 9.1 [(b) and (d)] for the deoxy- [(a) and (b)] and the CO-forms [(c) and (d)], and their pH difference spectra [(g) and (h)]. As spectra of Hb M Boston include the contributions from the ferric α- and ferrous β-hemes, it is difficult to distinguish between the two contributions. Since the contribution of the normal β-subunit to the spectra of Hb M Boston would be similar to that of Hb A, the RR spectra of Hb A were examined at the same conditions and their pH difference spectra (pH 7 minus pH 9) were calculated for the deoxy- and CO-forms as shown

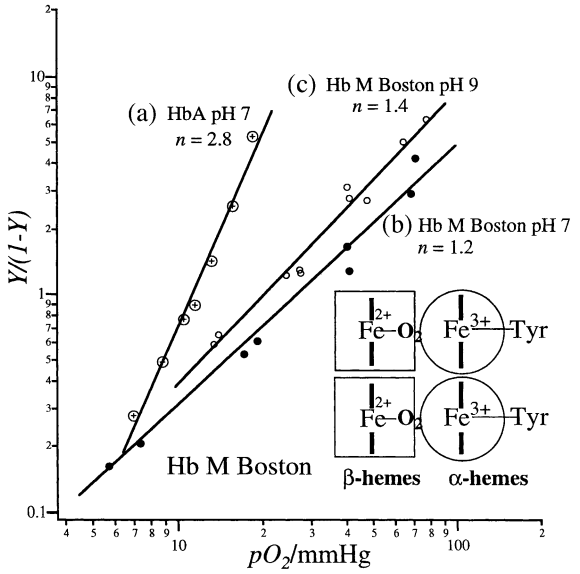

Fig. 3. Oxygen equilibrium curves of Hb A at pH 7 (a) and Hb M Boston at pH 7 (b) and pH 9 (c). Oxygen equilibrium curves were measured for Hb samples in 0.05 M Tris–Cl buffer containing 0.1 M NaCl at 25 °C. The concentrations of hemoglobin were 50 μM for Hb A and 60 μM (in heme) for Hb M Boston. The ratio of the population of the oxy- to deoxy-hemes (*Y*: fractional oxygen saturation) is plotted against the partial pressure of oxygen (P_{O_2}), both in logarithmic scales.

by spectra (e) and (f), respectively. The pH difference peak appeared only for the ν_4 mode in the case of Hb A [(e) and (f)] in contrast with the case of Hb M Boston which gave many difference peaks particularly for the CO-form (h). The additional difference peaks include those at 751, 1132, 1370, 1488 (1477), 1571 and 1626 (1613) cm^{-1} (parentheses mean negative peaks). The last four bands can be assigned to ν_4, ν_3, ν_2 and ν_{10} of a ferric heme, respectively [21–24]. Among them, the ν_3 and ν_{10} frequencies are sensitive to the coordination number of a heme, and the peak positions at 1477 and 1613 cm^{-1} at pH 9.0 are indicative of the six-coordinate high-spin (6c-hs) heme. The differences of the bands at 751 and 1132 cm^{-1} (Fig. 4h), which are also weakly present in the spectrum of Hb A (Fig. 4f), are assignable to ν_{15} and ν_{14}, respectively [25]. It is known that the abnormal subunit of Hb M Boston yields resonance enhanced Raman bands associated with the coordinated tyrosine upon excitation at 488.0 nm [21]. Therefore, Raman spectra excited at 488.0 nm were examined in this study again.

Fig. 5 shows the raw RR spectra of $\alpha_2^{Mmet}\beta_2^{deoxy}$ (a) and $\alpha_2^{Mmet}\beta_2^{CO}$ (b) of Hb M Boston, and deoxyHb A (c) and COHb A (d) all at pH 7.5 excited at 488.0 nm, and the corresponding pH 7.5 minus pH 9 difference spectra [(e), (f), (g) and (h)]. In the spectra of Hb M Boston there are several bands which are absent in the spectra of Hb A. These include the bands at 602, 795, 829, 876, 1278 and 1503 cm^{-1}. Some of them have been already assigned in the previous studies [21,26]; the 602 cm^{-1} band to the Fe(III)–O (tyrosinate) stretching (ν_{Fe-O}) [26], the 1278 cm^{-1} band to the C–O stretching mode (ν_{C-O}) of Tyrα58 [21], and the 1503 cm^{-1} band to Y19a [27]. The bands at 829 and 876 cm^{-1}, newly found in this experiment, are assignable to internal modes (possibly Y1 and overtone of Y16a) of the co-ordinated tyrosinate.

The pH difference spectra for deoxy- (Fig. 5g) and COHb A (Fig. 5h) yield no peak, indicating that the heme moiety undergoes no pH-dependent structural change. As to Hb M Boston, on the other hand, there is little difference in the RR spectra between pH 7 and 9 for $\alpha_2^{Mmet}\beta_2^{deoxy}$ (e), but are clearly different for $\alpha_2^{Mmet}\beta_2^{CO}$ (f). The differences are prominent for the bands at 602 (580), 754, 876, 1278, 1371, 1570 (1584) and 1627 (1605) cm^{-1} (parentheses mean the position of negative peaks). Most of these differences seem to appear from the ferric heme, but it is caused by CO binding to the ferrous β-heme. The low frequency shift of ν_{Fe-O} from 602 to 580 cm^{-1} means that the Fe(III)–O (tyrosinate) bond is somewhat weakened in $\alpha_2^{Mmet}\beta_2^{CO}$ at pH 9 than at pH 7 and would be compatible if Hisα87 is co-ordinated to the *trans* position of the Fe–O bond of the ferric α heme, giving rise to the 6c-hs structure. The decrease in Raman intensity of the ν_{C-O} mode at 1278 cm^{-1} at pH 9 also suggests some change in the Fe(III)-tyrosinate moiety. The differences at 1371, 1570 and 1627 cm^{-1} are considered to arise from the ν_4, ν_2 and ν_{10} modes of the ferric α-heme similar to the case of 413.1 nm excitation. While the ν_4 frequency is sensitive to π electron delocalization between Fe and the macrocycle, the

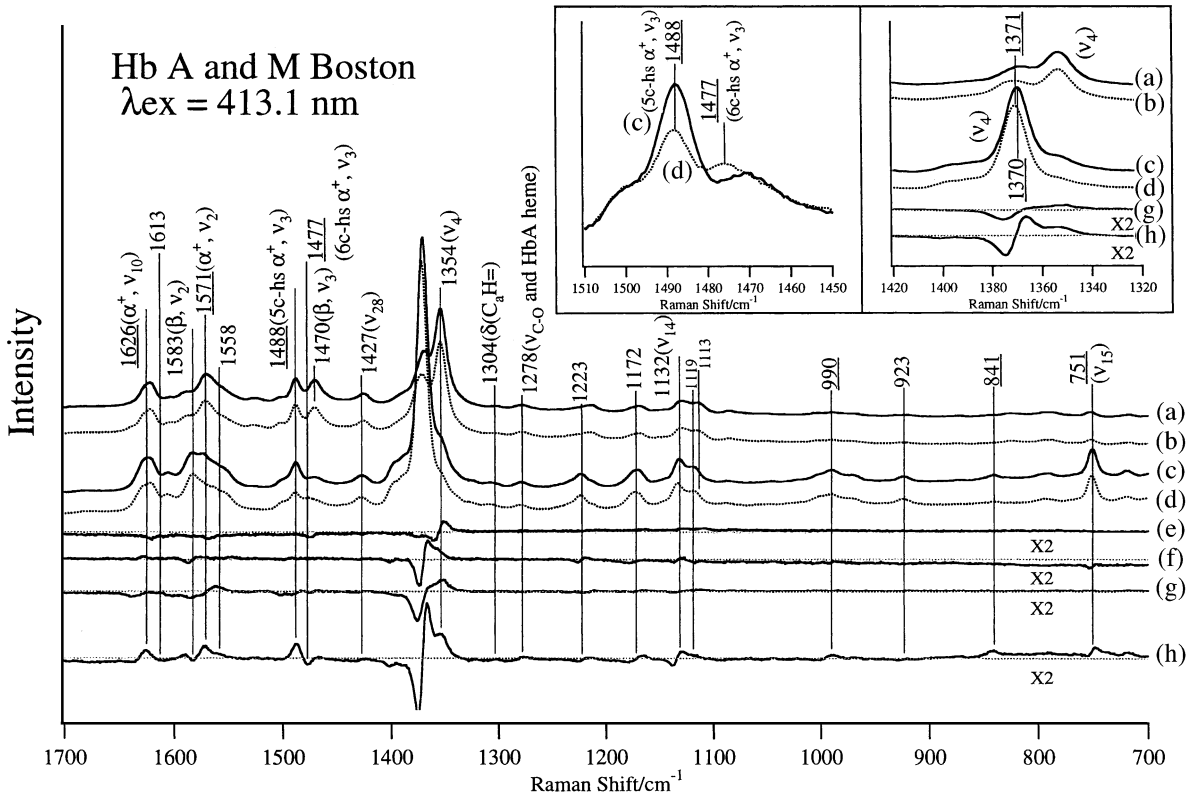

Fig. 4. The 413.1 nm excited RR spectra of $\alpha_2^{Mmet}\beta_2^{deoxy}$ at pH 7.3 (a), $\alpha_2^{Mmet}\beta_2^{deoxy}$ at pH 9.1 (b), $\alpha_2^{Mmet}\beta_2^{CO}$ at pH 7.3 (c), $\alpha_2^{Mmet}\beta_2^{CO}$ at pH 9.1 (d), and their difference spectra; (g) [(a) minus (b)], and (h) [(c) minus (d)]. Similar pH difference spectra (pH 7.1 minus pH 9.1) of deoxyHb A and COHb A are displayed by traces (e) and (f), respectively. The marker, α^+ means the α^{Mmet} heme throughout the figures. All samples are equilibrated with 0.05 M Tris–Cl buffer, containing 0.05 M Na_2SO_4 and 0.05 M NaCl. The concentration of Hb is 200 μM in heme. The ordinate scales of the difference spectra are expanded by a factor of two compared with those of raw spectra. The inset shows the expanded illustration of the spectra between 1320 and 1420 cm^{-1} (right) and 1450 and 1510 cm^{-1} (left).

ν_2 and ν_{10} frequencies are sensitive to the core size of the porphyrin and thus to the co-ordination number of Fe. Thus, the 488.0 nm excited Raman spectra as well as the 413.1 nm excited spectra support the idea that the coordination of axial ligands in the α heme is influenced by CO binding to the β heme through the subunit contacts.

Fig. 6 shows the 235 nm excited UVRR spectra for $\alpha_2^{Mmet}\beta_2^{deoxy}$ at pH 7.3 (a), $\alpha_2^{Mmet}\beta_2^{CO}$ at pH 7.3 (b), $\alpha_2^{Mmet}\beta_2^{deoxy}$ at pH 9.0 (c), $\alpha_2^{Mmet}\beta_2^{CO}$ at pH 9.0 (d), deoxyHb A at pH 7.3 (e), and COHb A at pH 9.0 (f) in the frequency region from 1700 to 700 cm^{-1}, and their differences, (g) [(a)−(b)], (h) [(c)−(d)], and (i) [(e)−(f)]. The 981 cm^{-1} band of SO_4^{2-} ions was used to normalize the intensity of the spectra [28]. In the spectrum of deoxyHb A, RR bands of tyrosine residues (Tyr) are seen at 1619 (Y8a), 1208 (Y7a), 1177 (Y9a) and 854 cm^{-1} (Y1), and those of tryptophan residues (Trp) are seen at 1558 (W3), 1360–1340 (W7; tryptophan doublet), 1011 (W16), 878 (W17) and 757 cm^{-1} (W18). The assignments are based on Harada et al. [27,29,30]. These UVRR spectra of Hb A excited at 235 nm are essentially the same as those excited at 229 nm [31], although relative intensities of bands are slightly different between them due to differences in resonance conditions.

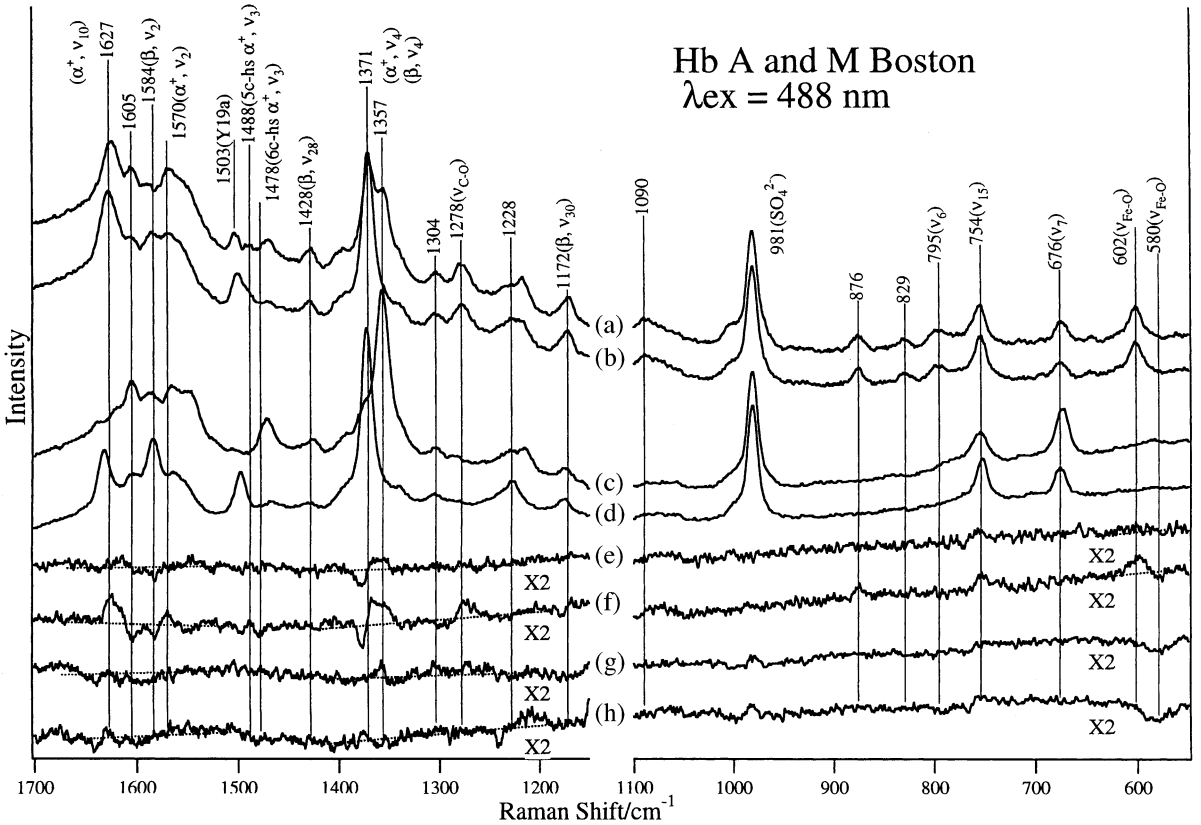

Fig. 5. The 488 nm excited RR spectra of Hb M Boston $\alpha_2^{Mmet}\beta_2^{deoxy}$ at pH 7.5 (a), and $\alpha_2^{Mmet}\beta_2^{CO}$ at pH 7.5 (b), and of deoxyHb A at pH 7.5 (c), and COHb A at pH 7.5 (d), and their difference spectra; (e) = $\alpha_2^{Mmet}\beta_2^{deoxy}$ at pH 7.5 (a) minus $\alpha_2^{Mmet}\beta_2^{deoxy}$ at pH 9.0, (f) = $\alpha_2^{Mmet}\beta_2^{CO}$ at pH 7.5 (b) minus $\alpha_2^{Mmet}\beta_2^{CO}$ at pH 9.0, (g) = deoxyHb A at pH 7.5 (c) minus deoxyHb A at pH 9.0, and (h) = COHb A at pH 7.5 (d) minus COHb A at pH 9.0. All samples are equilibrated with 0.05 M Tris–Cl buffer, containing 0.05 M Na_2SO_4 and 0.05 M NaCl. The concentration of Hb is 200 μM in heme.

The difference spectrum between deoxyHb A and COHb A indicates that the intensities of the W3, W16, W17 and W18 bands of Trp are much weaker for COHb A than for deoxyHb A, while the peak positions remain unaltered and that the frequencies of the Y8a and Y9a bands of Tyr are lower for COHb A than for deoxyHb A. These differences arise mainly from Trpβ37, Tyrα42, Tyrα140 and Tyrβ145 due to the quaternary structure change [13,32].

The difference spectrum between $\alpha_2^{Mmet}\beta_2^{deoxy}$ and $\alpha_2^{Mmet}\beta_2^{CO}$ of Hb M Boston is very small at pH 7.3. Magnitudes of the changes of Trp bands for Hb M Boston are 10–20% of those of Hb A, and the change of Tyr was negligible at pH 7.3. The change of Trp bands of Hb M Boston becomes a similar size to that of Hb A at pH 9.0, but the change in Tyr bands is still very small. This demonstrates that the quaternary structure change due to CO binding to the β heme is extremely small at pH 7.3, but becomes appreciable at pH 9.0 regarding Trp residues.

Fig. 7 shows the near-UV CD spectra of Hb A in the CO-, deoxy-, and met-forms (a), Hb M Boston in the CO- and deoxy-forms of the normal β subunit and in the met-form of the abnormal α subunit at pH 7 (b) and at pH 9 (c). As shown in Fig. 7a, deoxygenation is accompanied by a large decrease in the CD band of heme near 260 nm [33]. The band becomes further smaller in the met

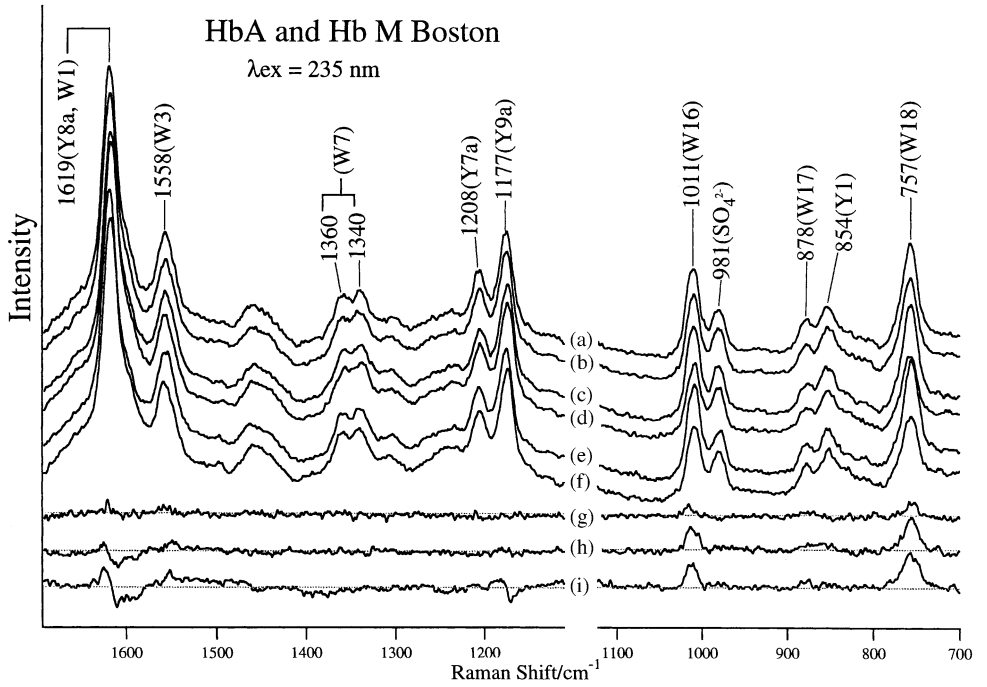

Fig. 6. The 235-nm excited UVRR spectra of Hb M Boston $\alpha_2^{Mmet}\beta_2^{deoxy}$ at pH 7.3 (a), $\alpha_2^{Mmet}\beta_2^{CO}$ at pH 7.3 (b), $\alpha_2^{Mmet}\beta_2^{deoxy}$ at pH 9.0 (c), $\alpha_2^{Mmet}\beta_2^{CO}$ at pH 9.0 (d), deoxyHb A (e) at pH 7.3, and COHb A (f) at pH 9.0, and their difference spectra; (g) [(a) minus (b)], (h) [(c) minus (d)], and (i) [(e) minus (f)]. All samples are equilibrated with 0.05 M Tris–Cl buffer, containing 0.1 M Na_2SO_4. The concentration of Hb is 200 μM in heme. Each spectrum is an average of 10 or 15 spectra. The ordinate scales of the difference spectra are the same as those of the raw spectra. The band marked by SO_4^{2-} means the totally symmetric stretching band of SO_4^{2-} ions. Although a strong broad band due to a synthetic quartz cell appeared between 800 and 900 cm^{-1}, its contribution is subtracted from the spectra shown here.

form. The 260 nm band of CO-bound Hb M Boston ($\alpha_2^{Mmet}\beta_2^{CO}$) was smaller than that of COHb A, and it becomes even smaller in the deoxy Hb M Boston ($\alpha_2^{Mmet}\beta_2^{deoxy}$) at both pH 7 and 9 (Fig. 7b,c).

Hb A shows a pronounced change in the CD spectrum of approximately 280–300 nm upon the T→R transition. The T-state Hb (deoxyHb A) exhibits a distinctive negative CD band, whereas the R-state Hb (oxy-, CO- or met-Hb A) gives weak positive CD bands. The change in ellipticity upon the T→R transition is considered to arise from local environmental changes of Tyrα42, Trpα37, and/or Tyrα140 [33–35]. Hb M Boston at pH 7 shows a distinctive negative CD band at 287 nm irrespective of CO binding to the normal β subunit, indicating that the quaternary structure of Hb M Boston is frozen in the T-state even for the ligand bound form of the normal β subunit. However, at pH 9, the negative band at 287 nm of deoxyHb M Boston ($\alpha_2^{Mmet}\beta_2^{deoxy}$) decreased markedly upon CO binding to the normal β subunit (Fig. 7c). This indicates that a quaternary structure does not change at pH 7 but appreciably changes at pH 9 upon ligand binding to the normal β subunit of Hb M Boston.

The inset of Fig. 7 shows the CD spectra of a model compound of tyrosine (*N*-acetyl-L-tyrosinamide) in water, that in 0.1 N NaOH, and *O*-phospho-L-tyrosine in 0.05 M Tris–Cl buffer, pH 7.2. Tyrosine in water gave a negative CD band at 274 and 280 nm, whereas deprotonated tyrosine (in alkaline) gave a positive CD band. The CD bands of phosphorylated tyrosine (Tyr-P) are also positive. These features remind us that Hb M Boston gives a broad positive band near 310 nm

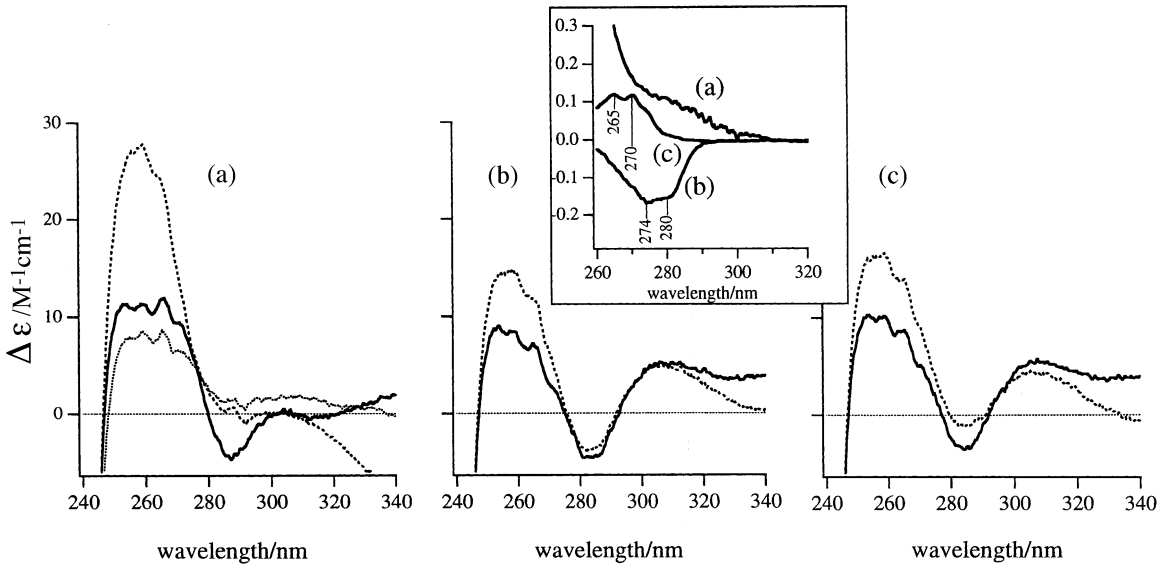

Fig. 7. Near-UV CD spectra of Hb A (a), Hb M Boston at pH 7 (b) and at pH 9 (c). Hb solution was 50 μM (in heme) in 0.05 M Tris–Cl buffer containing 0.1 M NaCl. Dotted line, CO-form; solid line, deoxy form. Thin dotted line in (a), met-form. For Hb M Boston, the deoxy and CO-forms mean $\alpha_2^{Mmet}\beta_2^{deoxy}$ and $\alpha_2^{Mmet}\beta_2^{CO}$, respectively. The inset shows the near-UV CD spectra of *N*-acetyl-L-tyrosinamide in 0.1 N NaOH (a), that in water (b) and *O*-phospho-L-tyrosine (Tyr-P) in 0.05 M Tris–Cl buffer, pH 7.2 (c). The sample concentrations are 0.9 mM for *N*-acetyl-L-tyrosineamide and 0.75 mM for *O*-phospho-L-tyrosine. CD spectra were acquired for a light path of 1 cm, and 40 scans were averaged.

in Fig. 7b,c. Although there are some differences in CD spectra between the model compounds and Tyr residue in the protein, it is likely that the positive CD band at 310 nm of Hb M Boston is due to Tyrα58 co-ordinated to the heme iron. The positive CD band of Hb M Boston at 310 nm did not change upon CO binding to the normal β subunit at pH 7 but decreased significantly at pH 9 (Fig. 7b,c), suggesting that Tyr co-ordination to the α heme was somehow perturbed by CO binding to the normal β subunit at pH 9.

4. Discussion

4.1. view=fitwidth,dpos=-1,id=H2 8,rid=H1 4Quaternary structure of $\alpha_2^{Mmet}\beta_2^{CO}$ at pH 7.5 and 9

We pointed out a local structure change around the ferric α-heme in $\alpha_2^{Mmet}\beta_2^{CO}$ of Hb M Boston. This change occurs in the CO bound form of β-heme and its magnitude is larger at pH 9.0 than at pH 7.5. This means that the intersubunit interactions are larger under alkaline conditions. Hb M Boston exhibits a low oxygen affinity and no cooperativity in the pH region between pH 6.5 and 7.9 [2]. Accordingly, it is considered that ligand binding does not induce the quaternary structure change for Hb M Boston in the pH region between pH 6 and 8. However, the oxygen affinity of Hb M Boston became higher above pH 8 and cooperativity appeared as demonstrated by Fig. 3. This new finding suggests melting of the frozen T structure upon deprotonation of some residue(s) at pH 9.

UVRR spectra reflect a higher order structure of protein. Here, the deoxy−CO difference spectrum of Hb A (Fig. 6i) is used as the standard of the T−R difference spectrum [13,19,32]. In the 235 nm excited UVRR spectra, the quaternary structure change appears as the spectral changes of Trp and Tyr residues. Fig. 6g reflects the quaternary structure change on CO binding to the ferrous β heme of Hb M Boston at pH 7.3. The difference in intensities of Trp bands are signifi-

cantly weak and no peak is observed for Tyr bands, indicating little change of a quaternary structure. However, the difference spectrum at pH 9 (Fig. 6h) is close to that of Hb A (Fig. 6i) except for the Y9a band. The quaternary structure-dependent UVRR spectral changes of Trp residues mainly (~70%) arise from Trpβ37 [13,36,37]. Accordingly, Trpβ37 changes toward a less hydrogen-bonding structure upon CO binding to the ferrous β-heme in a similar way to that in Hb A. Similar changes are also observed for other Hbs which cannot bind CO to the α heme, such as $\alpha_2^{NO}\beta_2^{deoxy}$ Hb [19] and $\alpha_2^{Ni}\beta_2^{deoxy}$ Hb [38]. The Y9a band did not change upon CO binding to Hb M Boston. The absence of the Y9a difference peak is also similar to the case of $\alpha_2^{Ni}\beta_2^{deoxy}$ Hb [38], in which a ligand cannot bind to the α heme. Thus, it is reasonable to conclude that the quaternary structure change occurs to Hb M Boston at pH 9 in a similar manner to that in ligand binding to the β heme of Hb A.

It is well known in the CD spectra that the negative band near 287 nm (Fig. 7a) serves as a T structure marker of Hb A [33]. As to Hb M Boston at pH 7, $\alpha_2^{Mmet}\beta_2^{CO}$ gives the T-structure marker in the same way as $\alpha_2^{Mmet}\beta_2^{deoxy}$, but the T structure marker of $\alpha_2^{Mmet}\beta_2^{CO}$ becomes significantly weaker at pH 9. This is consistent with the UVRR result in the sense that binding of CO to Hb M Boston yields a significant amount of R quaternary structure at pH 9.

4.2. What does occur in the α-heme upon CO binding to the β heme?

4.2.1. Absorption spectra

The pH differences in the absorption spectra shown in Fig. 2 indicate that pH dependence is larger for the CO-form than that for the deoxy form, although the spectral changes are qualitatively alike; the absorbance of the α ferric heme (406 nm) is larger at pH 7.5 than at pH 9.0, but that of the β ferrous heme (~420 nm) is opposite, and this trend is promoted by binding of CO to the β heme. In contrast, the pH difference spectra in the 480–620 nm region are qualitatively different between the deoxy and CO forms, although their magnitudes are small. The absorbance of $\alpha_2^{Mmet}\beta_2^{CO}$ at approximately 520 nm decreases at pH 9 than at pH 7.0, suggesting a decrease in the charge transfer interaction from the oxygen of Tyrα58 to Fe(III) at pH 9.0, while the interaction scarcely changes with pH for $\alpha_2^{Mmet}\beta_2^{deoxy}$. Plausible origins of this include elongation of the Fe(III)–O (Tyrα58) bond and an angle change of this bond with regard the heme normal. The former results in a decrease of the D parameter of EPR rhombicity, whereas the latter results in an increase of the E parameter. Whichever occurs, EPR rhombicity would increase.

4.2.2. Visible resonance Raman

Excitation of Raman spectra at 413.1 nm showed the ferric heme modes more favorably than ferrous heme modes. The frequencies of ν_3 and ν_{10} are known to be sensitive to the core size of porphyrin. The bands at 1488 (ν_3) and 1626 (ν_{10}) cm^{-1} are considered to reflect the five-coordinate high-spin (5c-hs) state [22–24]. This is also consistent with the fact that the corresponding marker bands of Fe(III)(PPIXDBE)($OC_6H_4NO_2$), a model compound of tyrosinate-coordinate heme, are observed at 1494 and 1630 cm^{-1}, respectively, (unpublished results). In the case of ferric hemes, the increase of core size occurs when the high-spin Fe atom is accommodated into the porphyrin plane by a change of the co-ordination number, and then the ν_3 and ν_{10} frequencies are expected to shift toward lower frequencies. The shift of ν_3 from 1488 to 1477 cm^{-1} and that of ν_{10} from 1626 to 1613 cm^{-1} in Fig. 4h is compatible to this idea. When the spin state is changed to a low spin upon a change of co-ordination number, then the core size becomes smaller, because the core size is in the order of 6c-hs > 5c-hs > 6c-ls [39].

The visible resonance Raman spectra excited at 488.0 nm provide information different from those excited at 413 nm, since there is a CT absorption from tyrosinate to Fe(III) near 488.0 nm [21]. The 488.0 nm excited Raman spectra of Hb M Boston showed obvious differences between pH 7.5 and 9.0 for $\alpha_2^{Mmet}\beta_2^{CO}$ as illustrated by Fig. 5f, but little difference for $\alpha_2^{Mmet}\beta_2^{deoxy}$ (Fig. 5e). The differences appeared mainly for the bands associated with the co-ordinated tyrosinate. Most important is the

frequency shift of the ν_{Fe-O} band from 602 to 580 cm^{-1}, meaning appreciable weakening of the Fe(III)-O (Tyrα58) bond at pH 9. Although either a movement of the oxygen of Tyrα58 or of Fe(III) can induce this, the movement of a high-spin Fe atom towards the porphyrin plane and the accompanied change in iron co-ordination number seems more likely judging from the core expansion mentioned above.

About the ν_{C-O} mode of tyrosinate at 1278 cm^{-1}, the Raman intensity for $\alpha_2^{Mmet}\beta_2^{CO}$ decreased at pH 9, but its frequency remained unchanged. A similar phenomenon occurs to the 876 cm^{-1} band of $\alpha_2^{Mmet}\beta_2^{CO}$, which presumably arises from the Y1 mode of the co-ordinated Tyr. Since Raman intensity reflects the electronic excited state and is approximately proportional to the square of absorbance at the wavelength of Raman excitation, but Raman frequencies reflect the electronic ground state, this observation conforms with the fact that the CT band becomes weaker at alkaline pH due to a change of the CT excited state. The difference peak at approximately 1370 cm^{-1} may mean that delocalization of d_π electrons of Fe(III) to the e_g orbital of porphyrin ring decreases even in the ground state and thus, ν_4 frequency is slightly raised at pH 9 than pH 7. All these observations imply appreciable reduction in the Fe(III)–tyrosinate interactions of the α heme at alkaline pH for the CO-bound form of β heme.

Thus, the Raman results suggest that the increased rhombicity (E/D) of the α heme of $\alpha_2^{Mmet}\beta_2^{CO}$ at pH 9 is caused by a decrease of the D parameter rather than an increase of the E parameter, and the decrease of the D parameter originated in weakening of the Fe(III)–O (Tyrα58) CT interactions and co-ordination of Hisα87 to its *trans* position. Since this is associated with binding of CO to the β heme, it should be regarded as an appearance of quaternary structure changes, although a route of communication remains to be clarified.

4.2.3. EPR spectra

The EPR spectral changes of the ferric α heme upon CO binding to the ferrous β-heme were clearly observed at pH 9.0, but not so clear at pH 7.5. The changes include the increase of anisotropy. The EPR anisotropy is usually represented in terms of the E/D value (rhombicity $= 300 \times E/D$), where D and E parameters reflect the axial (z) and the in-plane (x and y) ligand-field strengths, respectively, of the ferric α heme [40–42]. Increase of E means more degradation of tetragonal symmetry, while the decrease of D means weakening in electronic interactions of axial ligand(s) with Fe. Two sets of EPR signals with different values of rhombicity (6.7 and 3.5) were observed for $\alpha_2^{Mmet}\beta_2^{CO}$ at pH 9.0. The latter was the same as that for $\alpha_2^{Mmet}\beta_2^{CO}$ at pH 7.5. Since the in-plane vibrations of the α heme change little between pH 7.5 and 9.0, it is reasonable to ascribe the rhombicity change to a change of D rather than E.

Among Tyr-coordinated Fe(III) hemes, one may expect that H64Y mutant Mb is closest to the abnormal α-chain of Hb M Boston. However, the H64Y mutant of horse heart Mb (hhMb) adopts the 6c-hs state [43], different from the Hb M Boston in which the ferric α heme adopts the 5c-hs state [44]. Furthermore, for H64Y hhMb, were observed two sets of EPR signals with different values of rhombicity, 8.1 (main) and 3.0 (minor) [43]. In Hb M Saskatoon having abnormal β-chains, the 6c-hs heme gives a rhombicity of 8.1–8.7, whether the normal α-heme adopts the deoxy, ferrous-CO or ferric form [10,14]. Bovine liver catalase having a 5c-hs heme also gives rise to a similar value of rhombicity ($=7.5$) [45]. In contrast, Hb M Iwate, which has a 5c-hs heme in $\alpha_2^{Mmet}\beta_2^{deoxy}$ [21] and its fully oxidized form, $\alpha_2^{Mmet}\beta_2^{met}$ [26], gave a rhombicity of 2.4 for its CO form [46]. Thus, the co-ordination number of iron has no direct correlation with its value of rhombicity.

The Fe(III)–axial ligand distance may have some correlation with EPR anisotropy. According to the X-ray structural analysis of H64Y hhMb, the Fe-O (Tyr64) and the Fe–His bond-lengths are 218 and 229 pm, respectively, and the Fe atom is displaced toward Tyr64 from the plane of the pyrrole nitrogen atoms by 39 pm [43]. However, the EXAFS study of H64Y hhMb [47] gave a Fe–O distance of 188 pm, a value significantly shorter than the crystallographic value (218 pm), and inferred that the iron atom is displaced out of

the heme plane by 47 pm. These observations suggest that the heme structure is slightly different in crystal and solution. In the case of the H64Y mutant of sperm whale Mb (swMb), two kinds of Fe–O stretching bands have been observed at 578 and 600 cm^{-1} with nearly equal intensities in a solution state [48], and the former and latter bands were assigned to the 6c-hs and 5c-hs hemes, respectively. In this case, the 578 cm^{-1} component was correlated with the EPR minor component with rhombicity of 3.0, although differences between swMb and hhMb were noted there. Thus, interpretations are not always consistent. It seems to us more likely that the differences in temperatures are essential to make the population changes of the species in an equilibrium and thus, yields the accompanied differences in apparent observations. Namely, temperatures at which EPR, EXAFS and Raman were measured, are 4, 170 and 300 K, respectively, and seemingly the 6c-hs structure is more favorable at lower temperatures. The out-of-plane displacement of Fe atom would also depend on temperature. When the Fe atom comes into the heme plane, the Fe–O and Fe–His distances become longer and shorter, respectively, and the Fe–O stretching frequency as well as the *D* parameter of EPR would be altered even within the same co-ordination number.

The out-of-plane displacement of Fe(III) might determine rhombicity of heme EPR signals. It is generally thought that the Fe atom is displaced from the heme plane by approximately 50 pm in the N-bound 5c-hs hemes [49] and rhombicity is small ($\sim$3). This is also applicable to the O-coordinate 5c-hs hemes like Hb M Iwate and Hb M Boston. In bovine liver catalase with 5c-hs heme, rhombicity is 7.5 [45] and the displacement of the Fe(III) atom from the mean plane of all ring atoms is at most 20 pm [50–52]. This value of the out-of-plane displacement of Fe is smaller compared with those of many 5c-hs model compounds [49] and also than 47 pm of H64Y Mb [47]. If the co-ordination number of the main species is determined by a temperature-dependent equilibrium and the smaller values of the out-of-plane displacement of Fe give rise to the larger value of EPR rhombicity even in the five co-ordinate state, then all the existing data seem to be explained satisfactorily. Accordingly, we propose that the difference in rhombicity of the α ferric heme between pH 7.5 and 9.0 for the CO bound form of β-heme arises from differences in the out-of-plane displacement of Fe(III), that is, the Fe atom in the ferric α subunit is pushed into the heme plane by Tyr64 and/or pulled by Hisα87 more at pH 9.0 than at pH 7.5 due to the larger intersubunit interactions.

4.3. Communication pathway from the β-heme to the α-heme

Combination of information obtained from the measurements on oxygen equilibrium, EPR, CD and visible and UV resonance Raman, demonstrated that the frozen T structure of Hb M Boston is molten at pH 9 and that ligand binding to the β heme causes a quaternary structure change toward R. Upon this change, some structural change takes place in the α heme. Thus, the α heme has an interaction with the β heme through subunit interface as illustrated in Fig. 8. Similar phenomena occur on CO binding to the β-heme of $\alpha^{Ni}\beta^{deoxy}$ [38] and $\alpha^{NO}\beta^{deoxy}$ [19]. In both cases, Trpβ37 undergoes a change upon binding of a ligand to the β heme (Fig. 8), although the size of change depends on pH.

According to Perutz [6], CO binding to the α-heme pulls Fe(II) into the porphyrin plane and the F-helix of the α subunit is also pulled with the movement of the proximal His. The FG-corner of the α subunit connected to the F-helix of the α subunit has interaction with the C-helix of the β subunit through hydrogen bonds and electrostatic interactions. Trpβ37 belongs to the C-helix of the β subunit. Such a communication pathway of structural change from the α to β heme was previously suggested by Ho [53]. The change in the co-ordination number in the α-heme of Hb M Boston would be induced by the inverse process of this, that is the change of Trpβ37 finally causes the movement of Hisα87 of the F-helix of the α subunit. The amount of change is considered to be much smaller than that due to CO binding to the α heme in Hb A, but this small change of Hisα87 generates the 6c-hs ferric α-heme and thus, EPR spectral change.

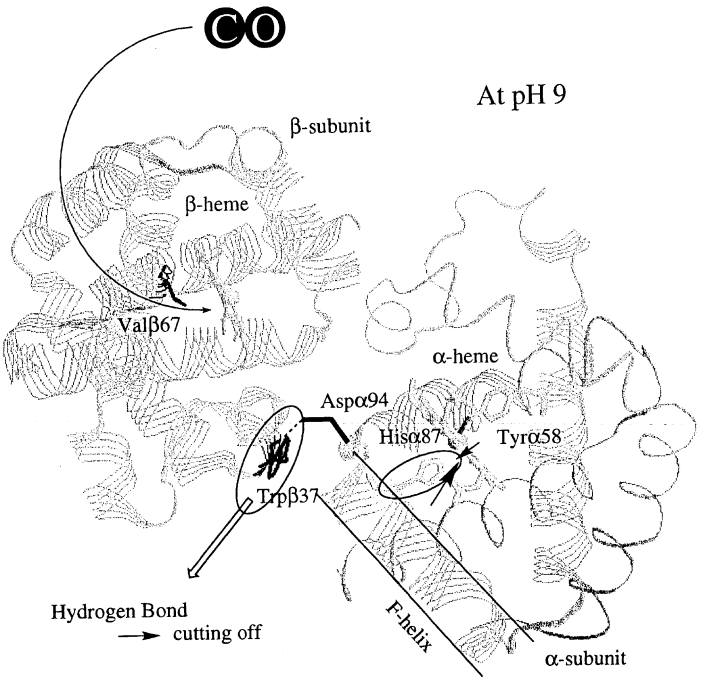

Fig. 8. Main chain arrangements in the α- and β-subunits of deoxyHb M Boston. Important amino acid residues discussed in this paper including Tyrα58, Hisα87, Aspα94 and Trpβ37 are explicitly designated. X-Ray crystallographic coordinates of the β-subunit are taken from Hb A [54], but those of the α-subunit are taken from the tyrosine mutant of horse myoglobin [43], registered in the Protein Data Bank and are rearranged partly. The thin broken line denotes the hydrogen bond between Trpβ37 and Aspα94, which is cleaved upon binding of CO to the β heme.

On the other hand, the UV spectral change of Tyr residues upon CO binding to the β heme of Hb M Boston is not so clear, and at least there is no change on Y7a and Y9a. This situation is similar to that in CO binding to the β heme of $\alpha_2^{Ni}\beta_2^{deoxy}$ [38], but not to that in CO binding to the β heme of $\alpha_2^{NO}\beta_2^{deoxy}$ for which the frequency shift toward the R state was observed for Y9a [19]. The Tyr residues which are responsible for UV Raman changes include Tyrα42, Tyrα140 and Tyrβ145 [32,38]. It is highly likely that this difference arises from the local structure of the distal side in the α-heme. The distal side of the α heme of $\alpha_2^{NO}\beta_2^{deoxy}$ contains a hydrogen bond between the heme-bound NO and Hisα58 (distal His). In contrast, the distal side in the α-heme of $\alpha_2^{Ni}\beta_2^{deoxy}$ involves no direct interaction between Ni and Hisα58. Hisα58 is contained in the E-helix and this residue is replaced by Tyr in the α subunit of Hb M Boston. Although Tyrα58 is co-ordinated to Fe(III), its ν_{CO} band was not affected by the quaternary structure change. Presumably, the E helix of the α subunit is perturbed insignificantly by binding of CO to the β heme similar to $\alpha_2^{Ni}\beta_2^{deoxy}$.

In conclusion, the α heme of Hb M Boston is influenced through the quaternary structure-dependent movement of Hisα87 and as a result, the Fe(III)–O (Tyrα58) bond was weakened by binding of CO to the β heme.

Acknowledgments

We thank Dr R. Jagenburg for his courtesy of giving us blood containing Hb M Boston. This study was supported by Grant-in-aid for Scientific Research on Priority Areas from the Ministry of Education, Sports, Culture, Science and Technology, Japan to M.N. (10670115) and T.K. (12045264).

References

[1] N. Hayashi, Y. Motokawa, G. Kikuchi, Studies on relationships between structure and function of Hemoglobin M_{Iwate}, J. Biol. Chem. 241 (1966) 79–84.

[2] T. Suzuki, A. Hayashi, Y. Yamamura, Y. Enoki, I. Tyuma, Functional abnormality of Hemoglobin M_{Osaka}, Biochem. Biophys. Res. Commun. 19 (1965) 691–695.

[3] T. Suzuki, A. Hayashi, A. Shimizu, Y. Yamamura, The oxygen equilibrium of Hemoglobin $M_{Saskatoon}$, Biochim. Biophys. Acta 127 (1966) 280–282.

[4] H.M. Ranney, R.L. Nagel, P. Heller, L. Udem, Oxygen equilibrium of Hemoglobin $M_{Hyde\ Park}$, Biochim. Biophys. Acta 160 (1968) 112–115.

[5] J. Monod, J. Wyman, J.-P. Changeux, On the nature of allosteric transition: a plausible model, J. Mol. Biol. 12 (1965) 88–118.

[6] M.F. Perutz, Stereochemistry of cooperative effects in haemoglobin, Nature 228 (1970) 726–739.

[7] M.F. Perutz, G. Fermi, B. Luisi, B. Shaanan, R.C. Liddington, Stereochemistry of cooperative mechanisms in hemoglobin, Acc. Chem. Res. 20 (1987) 309–321.

[8] J. Baldwin, C. Chothia, Haemoglobin: the structural changes related to ligand binding and its allosteric mechanism, J. Mol. Biol. 129 (1979) 175–220.

[9] T. Inubushi, M. Ikeda-Saito, T. Yonetani, Isotropically shifted NMR resonances for the proximal histidyl imidazole NH protons in cobalt hemoglobin and iron-cobalt hybrid hemoglobins. Binding of the proximal histidine toward porphyrin metal ion in the intermediate state of cooperative ligand binding, Biochemistry 22 (1983) 2904–2907.

[10] A. Hayashi, T. Suzuki, A. Shimizu, H. Morimoto, H. Watari, Changes in EPR spectra of M-type abnormal haemoglobins induced by deoxygenation and their implication for the haem–haem interaction, Biochim. Biophys. Acta 147 (1967) 407–409.

[11] L.W.-M. Fung, A.P. Minton, C. Ho, Nuclear magnetic resonance study of heme–heme interaction in Hemoglobin M Milwaukee: implications concerning the mechanism of cooperative ligand binding in normal hemoglobin, Proc. Natl. Acad. Sci. USA 73 (1976) 1581–1585.

[12] L.W.-M. Fung, A.P. Minton, T.R. Lindstrom, A.V. Pisciotta, C. Ho, Proton nuclear magnetic resonance studies of Hemoglobin M Milwaukee and their implications concerning the mechanism of cooperative oxygenation of hemoglobin, Biochemistry 16 (1977) 1452–1462.

[13] M. Nagai, S. Kaminaka, Y. Ohba, Y. Nagai, Y. Mizutani, T. Kitagawa, Ultraviolet resonance Raman studies of quaternary structure of hemoglobin using a tryptophan β37 mutant, J. Biol. Chem. 270 (1995) 1636–1642.

[14] K. Nishikura, Y. Sugita, M. Nagai, Y. Yoneyama, Ethylisocyanide equilibria of Hemoglobins M Iwate, M Boston, M Hyde Park, M Saskatoon, and Milwaukee-I in half-ferric and fully reduced states, J. Biol. Chem. 250 (1975) 6679–6685.

[15] K. Nagai, H. Hori, The influence of quaternary structure on the EPR spectra of ferric haemoglobin, FEBS Lett. 93 (1978) 275–277.

[16] S. Kaminaka, T. Kitagawa, A novel idea for practical UV resonance Raman measurement with a double monochromator and its application to protein structural studies, Appl. Spectrosc. 46 (1992) 1804–1808.

[17] S. Kaminaka, T. Kitagawa, Novel spinning cell system for UVRR measurements of powder and small-volume solution samples in back-scattering geometry: application to solid tryptophan and mutant hemoglobin solution, Appl. Spectrosc. 49 (1995) 685–687.

[18] S. Song, S.A. Asher, Internal intensity standards for heme protein UV resonance Raman studies: excitation profiles of cacodylic acid and sodium selenate, Biochemistry 30 (1991) 1199–1205.

[19] S. Nagatomo, M. Nagai, A. Tsuneshige, T. Yonetani, T. Kitagawa, UV resonance Raman studies of α-nitrosyl hemoglobin derivatives: relation between the α1-β2 subunit interface interactions and the Fe-histidine bonding of α heme, Biochemistry 38 (1999) 9659–9666.

[20] Y. Sugita, Y. Yoneyama, Oxygen equilibrium of hemoglobins containing unnatural hemes, J. Biol. Chem. 246 (1971) 389–394.

[21] K. Nagai, T. Kagimoto, A. Hayashi, F. Taketa, T. Kitagawa, Resonance Raman studies of Hemoglobins M: evidence for iron-tyrosine charge–transfer interactions in the abnormal subunits of Hb M Boston and Hb M Iwate, Biochemistry 22 (1983) 1305–1311.

[22] T.G. Spiro, J.D. Stong, P. Stein, Porphyrin core expansion and doming in heme proteins. New evidence from resonance Raman spectra of six-coordinate high-spin iron(III) hemes, J. Am. Chem. Soc. 101 (1979) 2648–2655.

[23] J. Teraoka, T. Kitagawa, Raman characterization of axial ligands for penta- and hexacoordinate ferric high- and intermediate-spin (octaethylporphyrinato)iron(III) complexes. Elucidation of unusual resonance Raman spectra of cytochrome *c*′, J. Phys. Chem. 84 (1980) 1928–1935.

[24] Y. Ozaki, K. Iriyama, H. Ogoshi, T. Ochiai, T. Kitagawa, Resonance Raman characterization of iron–chlorin complexes in various spin, oxidation, and ligation states. 1. Comparative study with corresponding iron–porphyrin complexes, J. Phys. Chem. 90 (1986) 6105–6112.

[25] S. Hu, K.M. Smith, T.G. Spiro, Assignment of protoheme resonance Raman spectrum by heme labeling in myoglobin, J. Am. Chem. Soc. 118 (1996) 12638–12646.

[26] M. Nagai, Y. Yoneyama, T. Kitagawa, Characteristics in tyrosine coordinations of four Hemoglobins M probed by resonance Raman spectroscopy, Biochemistry 28 (1989) 2418–2422.

[27] I. Harada, T. Miura, H. Takeuchi, Origin of the doublet at 1360 and 1340 cm^{-1} in the Raman spectra of tryptophan and related compounds, Spectrochim. Acta 42A (1986) 307–312.

[28] J.M. Dudik, C.R. Johnson, S.A. Asher, Wavelength dependence of the preresonance Raman cross sections of CH_3CN, SO_4^{2-}, ClO_4^- and NO_3^-, J. Chem. Phys. 82 (1985) 1732–1740.

[29] T. Miura, H. Takeuchi, I. Harada, Characterization of individual tryptophan side chain in proteins using Raman spectroscopy and hydrogen–deuterium exchange kinetics, Biochemistry 27 (1988) 88–94.

[30] T. Miura, H. Takeuchi, I. Harada, Tryptophan Raman bands sensitive to hydrogen bonding and side-chain conformation, J. Raman Spectrosc. 20 (1989) 667–671.

[31] L.A. Dick, G. Heibel, E.G. Moore, T.G. Spiro, UV resonance Raman spectra reveal a structural basis for diminished proton and CO_2 binding to α,α-cross-linked hemoglobin, Biochemistry 38 (1999) 6406–6410.

[32] M. Nagai, H. Wajcman, A. Lahary, T. Nakatsukasa, S. Nagatomo, T. Kitagawa, Quaternary structure sensitive tyrosine residues in human hemoglobin: UV resonance Raman studies of mutants at α140, α35, and β145 tyrosine, Biochemistry 38 (1999) 1243–1251.

[33] M.F. Perutz, J.E. Ladner, S.R. Simon, C. Ho, Influence of globin structure on the state of the heme. I. Human deoxyhemoglobin, Biochemistry 13 (1974) 2163–2173.

[34] M.F. Perutz, A.R. Fersht, S.R. Simon, G.C.K. Roberts, Influence of globin structure on the state of the heme. II. Allosteric transitions in methemoglobin, Biochemistry 13 (1974) 2174–2186.

[35] R. Li, Y. Nagai, M. Nagai, Contribution of α140Tyr and β37Trp to the near-UV CD spectra on quaternary structure transition of human Hemoglobin A, Chirality 12 (2000) 216–220.

[36] K.R. Rodgers, C. Su, S. Subramaniam, T.G. Spiro, Hemoglobin R–T structural dynamics from simultaneous monitoring of tyrosine and tryptophan time-resolved UV resonance Raman signals, J. Am. Chem. Soc. 114 (1992) 3697–3709.

[37] M. Nagai, K. Imai, S. Kaminaka, Y. Mizutani, T. Kitagawa, Ultraviolet resonance Raman studies of hemoglobin quaternary structure using a tyrosine-α42 mutant: changes in the $\alpha_1\beta_2$ subunit interface upon the T–R transition, J. Mol. Struct. 379 (1996) 65–75.

[38] S. Nagatomo, N. Shibayama, M. Nagai, T. Kitagawa, Differences in changes of the α1-β2 subunit contacts between ligand binding to the α_1 and β_2 subunits of hemoglobin A: UV resonance Raman analysis using Ni–Fe hybrid hemoglobin, to be published.

[39] A. Boffi, T.K. Das, S.della Longa, C. Spagnuolo, D.L. Rousseau, Pentacoordinate hemin derivatives in sodium dodecyl sulfate micelles: model systems for the assignment of the fifth ligand in ferric heme proteins, Biophys. J. 77 (1999) 1143–1149.

[40] S. Mizuhashi, Anisotropy of *g*-values in low-spin ferrihaemoglobin azide, J. Phys. Soc. Jpn. 26 (1969) 468–492.

[41] M. Kotani, On the electronic state of iron in hemoglobins, with a short introduction to problems of quantum biophysics, Rev. Mod. Phys. 35 (1963) 717–720.

[42] G. Palmer, in: D. Dolphin (Ed.), The Porphyrins, vol. IV, Academic Press, New York, 1979, pp. 313–354.

[43] R. Maurus, R. Bogumil, Y. Luo, et al., Structural characterization of heme ligation in the His64→Tyr variant of myoglobin, J. Biol. Chem. 269 (1994) 12606–12610.

[44] P.D. Pulsinelli, M.F. Perutz, R.L. Nagel, Structure of Hemoglobin M Boston, a variant with a five-coordinated ferric heme, Proc. Natl. Acad. Sci. USA 70 (1973) 3870–3874.

[45] K. Torii, Y. Ogura, Electron paramagnetic resonance study of bovine liver catalase, J. Biochem. 65 (1969) 825–827.

[46] A. Hayashi, A. Shimizu, Y. Yamamura, H. Watari, Electron spin resonance of Haemoglobin M_{Iwate} and M_{Osaka}, Biochim. Biophys. Acta 102 (1965) 626–628.

[47] H.-L. Tang, B. Chance, A.G. Mauk, L.S. Powers, K.S. Reddy, M. Smith, Spectroscopic, electrochemical, and ligand binding properties of the horse heart metmyoglobin His64→Tyr variant, Biochim. Biophys. Acta 1206 (1994) 90–96.

[48] K.D. Egeberg, B.A. Springer, S.A. Martinis, S.G. Sligar, D. Morikis, P.M. Champion, Alteration of sperm whale myoglobin heme axial ligation by site-directed mutagenesis, Biochemistry 29 (1990) 9783–9791.

[49] J.L. Hoard, M.J. Hamor, T.A. Hamor, W.S. Caughey, The crystal structure and molecular stereochemistry of methoxyiron(III) mesoporphyrin-IX dimethyl ester, J. Am. Chem. Soc. 87 (1965) 2312–2319.

[50] T.J. Reid, M.R.N. Murthy, A. Sicignano, N. Tanaka, W.D.L. Musick, M.G. Rossmann, Structure and heme environment of beef liver catalase at 2.5 Å resolution, Proc. Natl. Acad. Sci. USA 78 (1981) 4761–4771.

[51] I. Fita, A.M. Silva, M.R.N. Murthy, M.G. Rossmann, The refined structure of beef liver catalase at 2.5 Å resolution, Acta Crystallogr. B 42 (1986) 497–515.

[52] I. Fita, M.G. Rossmann, The active center of catalase, J. Mol. Biol. 185 (1985) 21–37.

[53] C. Ho, Proton nuclear magnetic resonance studies on hemoglobin: cooperative interactions and partially ligated intermediates, Adv. Protein Chem. 43 (1992) 152–312.

[54] G. Fermi, M.F. Perutz, B. Shaanan, R. Fourme, The crystal structure of human deoxyhaemoglobin at 1.74 Å resolution, J. Mol. Biol. 175 (1984) 159–174.